Adv. Radio Sci., 6, 315–318, 2008
www.adv-radio-sci.net/6/315/2008/

Advances in Radio Science

Cloud physical properties and empirical polarimetric measurements of rain signatures at C-Band

J. Steinert and M. Chandra

Professur für Hochfrequenztechnik und Photonik, Technische Universität Chemnitz, Germany

Abstract. Raindrops are one type of precipitation in stratiform and convective clouds. To get relationships for describing the raindrops two different methods were used. In the first way, the microphysical properties of the liquid hydrometeors were examined. For this the use of the Rayleigh approximation for small particles (raindrops at C-Band) and the drop size distribution by Ulbrich (Γ-DSD) lead to the calculation of the reflectivity at horizontal polarisation Z_{HH}, the reflectivity at vertical polarisation Z_{VV} and the differential reflectivity Z_{DR}. In the second way, rain signatures were separated from polarimetric measurements. The database of these measurements consists of datasets measured by the dual polarimetric C-Band weather radar POLDIRAD (DLR, Oberpfaffenhofen). The aim of this study was then to combine and to compare the results from the real radar measurements against the theoretical calculations in the $Z_{HH}-Z_{DR}$ plane. Based on these observations and calculations, scientific results for future practical use will be presented in form of empirical equations including $Z_{HH}-Z_{DR}$. Finally in form of scientific discussion, the $Z_{HH}-Z_{DR}$ plane will be critically assessed for outstanding problems or issues.

1 Introduction

The microphysical structure of clouds is depending on the type of hydrometeors that are inside. In a previous step of a hydrometeor classification a separation in stratiform (or rain) clouds and convective (or thunderstorm) clouds has to be done. The existence of a melting band will be considered as criterion for discrimination between the two types of clouds. This transistion zone of frozen and liquid hydrometeors is typically present in stratiform events. A further look needs to be taken on the shape of the raindrops. The shape is obviously oblate but the correct equation for the relation between the axes of the spheroid is variable.

Correspondence to: J. Steinert
(joerg.steinert@etit.tu-chemnitz.de)

The paper starts in Sect. 2 with a short description of the scattering theory of raindrops. In the following Sect. 3, the analysis of the empirical results from dual polarimetrical radar measurements will be treated. The combination of the two approaches and the results of the comparison are shown in Sect. 4.

2 Microphysical simulation

2.1 Theory

Raindrops can be modelled as oblate spheroids. The result is that the backscattered signal (represented by the backscattering cross section BCS) in horizontal polarisation is larger than the backscattered signal in vertical polarisation. In addition the weather radar measures the backscattered power of a scattering pulse volume and not single points in the atmosphere. Because of this, the calculation of the reflectivity has to include the numbers of drops per unit volume (drop size distribution DSD). To distinguish the differential reflectivity, two parameters are relevant. Firstly the canting angle, which is assumed as a constant value at 90 degrees (horizontally aligned drops), and secondly the geometrical relation between the horizontal and and the vertical dimension of the drops. This relation is also called axial ratio AR and is described with the drop size relation (DSR).

2.1.1 Backscattering cross section

Raindrops consist of liquid water. Therefore, the results of Ray (1972) for water were implemented to calculate the refractive index. For the BCS of a single raindrop the Rayleigh approximation was assumed. Oguchi (1983) described well the calculation sequence for the BCS ($\sigma_{HH,VV}$ in mm^2) therefore it won't be elaborated here. The calculation of $\sigma_{HH,VV}$ includes the usage of the refractive index and the DSR. The DSR builds the connection between the axis ratio AR of the raindrop and the equivolumetric diameter D_e (the diameter of a sphere with the same volume as the spheroid).

Published by Copernicus Publications on behalf of the URSI Landesausschuss in der Bundesrepublik Deutschland e.V.

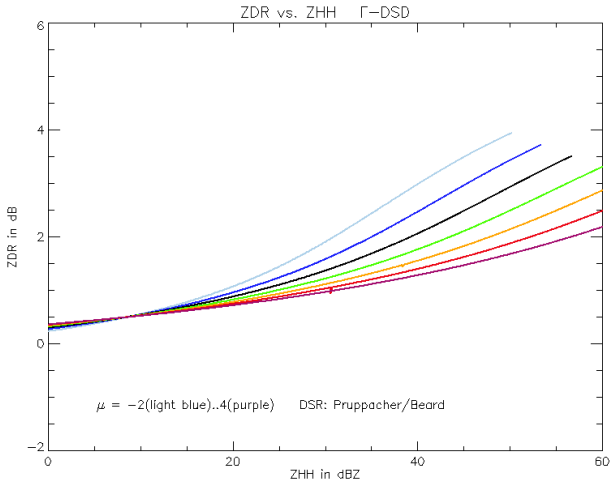

Fig. 1. Γ-DSD with Pruppacher/Beard DSR.

There are several equations to describe the shape of a raindrop. Often used is the DSR by Pruppacher and Beard (1970)

$$AR = 1.03 - 0.62 \cdot D_e \tag{1}$$

with D_e in cm and AR defined as the ratio between the minor axis and the major axis of an oblate spheroid.

2.1.2 Drop size distribution

The distribution of raindrops in a scattering volume can be described by an exponential distribution (e.g., Marshall and Palmer, 1948) or more in general with the Γ-DSD by Ulbrich (1983). The difference is that the Γ-DSD has the additional parameter μ[1]. The following equations (Eqs. 2 to 6) are taken from the paper of Ulbrich (1983).

$$N(D_e) = N_0 \cdot (D_e)^{\mu} \cdot e^{-\Lambda \cdot D_e} \tag{2}$$

with

$$N_0 = 1.52 \cdot 10^4 \cdot e^{3.14\mu} \tag{3}$$

and $\Lambda = \frac{3.67+\mu}{D_0}$.

In the equations above $N(D_e)$ is in $cm^{-1} \cdot m^{-3}$, N_0 is in $cm^{-1-\mu} \cdot m^{-3}$ and the unit of the median diameter D_0 is cm. If μ is set to 0 the Γ-DSD transforms to an exponential distribution.

D_0 is related to the rainrate R with

$$D_0 = \epsilon \cdot R^{\delta} \tag{4}$$

where

$$\epsilon = (3.67 + \mu)[33.31 \cdot N_0 \cdot \Gamma(4.67 + \mu)]^{\frac{-1}{4.67+\mu}} \tag{5}$$

[1] μ is related to the shape of the DSD.

and

$$\delta = \frac{1}{4.67 + \mu}. \tag{6}$$

The three equations (Eqs. 4, 5 and 6) will be used to calculate the rainrates of the simulation results in Sect. 4.

2.1.3 Reflectivity

The reflectivity in the horizontal polarisation z_{HH} and in the vertical polarisation z_{VV} can be calculated by Eq. 7.

$$z_{HH,VV} = \frac{\lambda^4}{\pi^5 \cdot |K|^2} \cdot \int_{D_e} \sigma_{HH,VV}(D_e) \cdot N(D_e) dD_e \tag{7}$$

with the wavelength λ of the transmitted/received signal, K the dielectric factor calculated by: $K = \frac{\epsilon-1}{\epsilon+2}$ and the complex permittivity ϵ. Because of the high dynamic range of the reflectivity values from Eq. 7, the transformation into the logarithmic scale is obvious with: $Z_{HH,VV} = 10 \cdot log_{10}(z_{HH,VV})$. The Unit of $Z_{HH,VV}$ is dBZ (mention the capitalization of Z).

The differential reflectivity Z_{DR} that is related to the shape of the hydrometeors is then estimated with

$$Z_{DR} = Z_{HH} - Z_{VV}. \tag{8}$$

The result of the simulation of Z_{HH} and Z_{DR} for raindrops is shown in Fig. 1. For this simulation the DSR of Pruppacher and Beard (1970) and the Γ-DSD of Ulbrich (1983) were used. The shape parameter μ of the DSD were varied in steps of 1 between -2 and 4.

3 Empirical results

In a previous work (Steinert and Chandra (2007)) polarimetrical weather radar data from the POLDIRAD (Oberpfaffenhofen, Germany) were analysed. The POLDIRAD is a dual polarimetrical radar and gives the opportunity to measure the co-polar and the cross-polar echoes from an illuminated pulse volume. The operating frequency is at C-Band with a wavelength of 5.45 cm. More detailed information of the radar hardware is available in Schroth et al. (1988). The analysis of the data in Steinert and Chandra (2007) was based on the measurements at the reflectivity in horizontal polarisation Z_{HH} and the differential reflectivity Z_{DR}. These two polarimetric parameters were combined to describe the results for raindrops.

3.1 Selecting the data

The data basis consists of reflectivity values from manual selected areas of raindrops. For this the datasets were separated into stratiform clouds and convective clouds. Then the rain signatures from different weather events for both types of clouds were analysed.

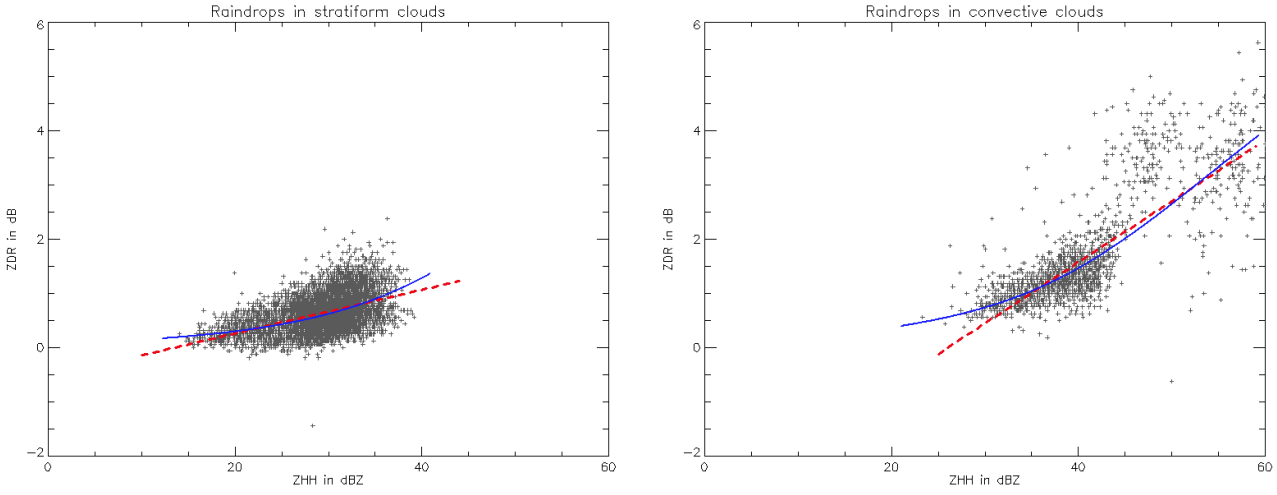

Fig. 2. Z_{DR}-Z_{HH}-plot of the selected data with the fitted functions (dashed red lines) and the microphysical simulation (blue curves)-left: stratiform clouds, right: convective clouds.

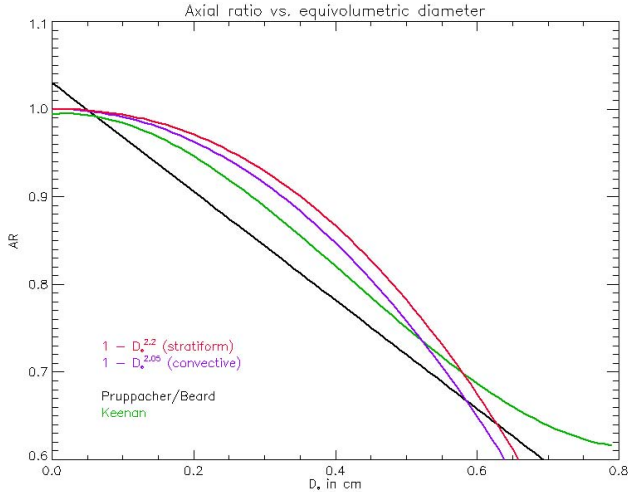

Fig. 3. DSR from literature (black and green) in comparison to empirical DSR (red and purple).

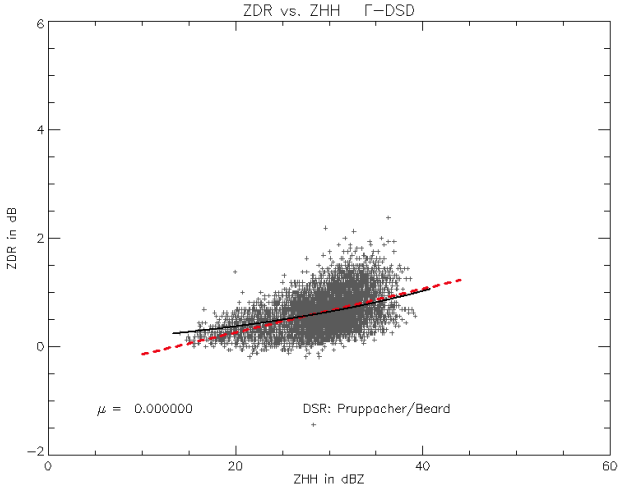

Fig. 4. Data points (dark grey) with simulation result (black curve) and empirical fit (red dashed line) for the DSR of Pruppacher and Beard (1970) and stratiform events in the Z_{DR} vs. Z_{HH} plane.

3.2 Fitting the data

The selected data of Z_{HH} in dBZ and Z_{DR} in dB were fitted with linear functions. The function and the data for the stratiform case are shown on the left in Fig. 2 and the fit is decribed with:

$$Z_{DR} = 0.04 \cdot Z_{HH} - 0.51 \quad (9)$$

For the convective case the fit corresponds to Eq. 10. In Fig. 2 on the right side the data is overplotted with the fit.

$$Z_{DR} = 0.11 \cdot Z_{HH} - 2.93 \quad (10)$$

The differences in the Eqs. (9) and (10) show that the separation of the raindrops with respect to the origin (stratiform or convective) is useful.

4 Combination of microphysical properties with empirical results

The microphysical simulation of the backscattered signal from raindrops have two degrees of freedom. These are the DSR and the DSD of the raindrops in the scattering volume.

Table 1. D_0 and rainrate of the microphysical simulations in Figs. 2 and 4.

Event	D_0 in mm	R in $\frac{mm}{hr}$
stratiform (empirical DSR)	0.75 .. 1.9	0.10 .. 7.39
stratiform (Prupp./Beard DSR)	0.4 .. 1.1	0.24 .. 26.5
convective (empirical DSR)	1.0 .. 3.5	0.37 .. 128.2

For the comparison of the empirical fitting function with the simulation a least square fit algorithm was used. This lead to the result that the DSR of Pruppacher and Beard (1970) or other DSR (e.g., Keenan et al., 2001 or Beard and Chuang, 1987) deliver weak results. The analysis led us to propose that the DSR should have the form: $AR{=}1{-}(D_e)^b$ with b close to 2. Furthermore the results for the DSR are different for stratiform clouds and convective clouds. The investigated DSR is described for stratiform events by

$$AR = 1 - (D_e)^{2.2} \tag{11}$$

and for convective events by

$$AR = 1 - (D_e)^{2.05} \tag{12}$$

with D_e in cm.

In Fig. 3 the DSR of Pruppacher and Beard (1970) (black line), Keenan et al. (2001) (green line) are shown together with the investigated DSR for raindrops from stratiform events (Eq. 11, red line) and from convective events (Eq. 12, purple line).

In the Γ-DSD μ was set to 0 so that the Γ-DSD transforms to an exponential distribution. At the first stage the parameter N_0 was fixed at the given value of Ulbrich (1983) (Eq. 3) with $\mu{=}0$ so $N_0{=}1520\,mm^{-1}{\cdot}m^{-3}$. The simulation results are displayed in Fig. 2 for the stratiform case (left plot in the figure) and for the convective events (right plot in the figure) with blue curves. For comparison the empirical fitting functions are shown in red dashed lines and the data were plotted with dark grey points.

The usage of the popular DSR of Pruppacher and Beard (1970) (Eq. 1) is displayed as an example for stratiform events in Fig. 4. The difficulty that comes along with this DSR is, that N_0 of the DSD has to be adjusted to $N_0{=}70\,000\,mm^{-1}\cdot m^{-3}$. This value is too high in comparison to the literature (e.g., Ulbrich, 1983 and Marshall and Palmer, 1948).

Corresponding ranges of D_0 and the calculated rainrate (cf., Eqs. 4, 5 and 6) are listed in Table 1. The usage of the DSR by Pruppacher and Beard (1970) lead to higher rainrates (cf., row 1 and 2 in Table 1).

5 Conclusions

The simulation of the reflectivity for pulse volumes including raindrops was presented. The difficulties are the parameters to "adjust" the DSD and therewith the calculation of the reflectivity. This parameters are namely μ, N_0 and the DSR. The DSD values (μ and N_0) were fixed and so just the DSR played a role for the analysis. The empirical DSR of Eqs. 11 and 12 give good results in comparison to the measured data (Sect. 3). With the DSR of Pruppacher and Beard (1970) the comparison was just useful with a change of N_0 to an extraordinary value. The calculated rainrates (Table 1) that corresponds to the simulation results can't be compared correctly due to nonexisting rainrate measurements for the observed weather events. A future topic will be the implementation of the results in a hydrometeor classification algorithm.

References

Beard, K. V. and Chuang, C.: A new model for the equilibrium shape of raindrops, J. Atmos. Sci., 44, 1509–1524, 1987.

Keenan, T., Carey, L., Zrnic, D., and May, P.: Sensitivity of 5-cm wavelength polarimetric radar variables to raindrops axial ratio and drop size distribution, J. Appl. Meteorol., 40, 526–545, 2001.

Marshall, J. and Palmer, W.: The distribution of raindrops with size, J. Meteorol., 5, 165–166, 1948.

Oguchi, T.: Electromagnetic wave propagation and scattering in rain and other hydrometeors, Proceedings of the IEEE, 71, 1029–1078, 1983.

Pruppacher, H. and Beard, K. V.: A wind tunnel investigation of the internal circulation and shape of water drops falling at terminal velocity in air, Q. J. Roy. Meteorol. Soc., 96, 247–256, 1970.

Ray, P. S.: Broadband complex refractive indices of ice and water, Appl. Optics, 11, 1836–1844, 1972.

Schroth, A. C., Chandra, M. S., and Meischner, P. F.: A C-Band Coherent Polarimetric Radar for Propagation and Cloud Physics Research, J. Atmos. Ocean. Technol., 5, 803–822, 1988.

Steinert, J. and Chandra, M.: Reflectivity relationships of polarimetric C-band measurements of rain signatures, Proceedings of WFMN07, 30–34, http://archiv.tu-chemnitz.de/pub/2007/0210/, 2007.

Ulbrich, C. W.: Natural variations in analytical form of the raindrop size distribution, J. Clim. Appl. Meteorol., 22, 1764–1775, 1983.